Asian Journal of Physics
Vol. 31, No 2 (2022) 195-208
Available on: www.asianjournalofphysics.com

ap

Biopolymers in the eggshell of the Argentine Black and White Tegu (*Salvator merianae*): a Raman microscopy study

Rosa María Susana Álvarez[1,2], Alfredo Nicolás Dominguez[1], Francisco Alejandro Cortez[3], Oscar Augusto Carlino-Aráoz[4], and Fernando Horacio Campos-Casal[3]

[1] *Instituto de Química del Noroeste Argentino* (*INQUINOA*), *CONICET-UNT, Ayacucho 471, San Miguel de Tucumán, CP 4000, Tucumán, Argentina.*

[2] *Instituto de Química Física, Facultad de Bioquímica, Química y Farmacia, Universidad Nacional de Tucumán, San Lorenzo 456, San Miguel de Tucumán, T4000CAN, Tucumán, Argentina.*

[3] *Cátedra de Biología del Desarrollo, Facultad de Agronomía y Zootecnia, Universidad Nacional de Tucumán. Florentino Ameghino S/N, El Manantial, T4104AUD, Tucumán, Argentina.*

[4] *Cátedra de Histología Veterinaria, Facultad de Agronomía y Zootecnia, Universidad Nacional de Tucumán. Av. Pres. Néstor Kirchner 1900, San Miguel de Tucumán, T4000CAN, Tucumán, Argentina.*

The Argentine Black and White Tegu *Salvator merianae* is one of the largest South American lizards. The eggs of this reptile, whitish in color and oval in shape, are soft and resistant but permeable to water, evidencing interesting properties to be exploited in the field of biomaterial engineering. This is the first study focused on the organic matrix of the *Salvator merianae* eggshell. The structural analysis, carried out by Raman microscopy and complemented with transmission electron microscopy and with brightfield and polarized light optical microscopy, reveals an interesting organization of fibrillar polymers. The spatial distribution of collagen and keratins correlates with the morphology of this extraordinary complex system.

Keywords: Collagen, Keratin, Biopolymers, Soft eggshell.

1 Introduction

The biodiversity of reptiles is associated with a remarkable heterogeneity of reproductive patterns and adaptive strategies that allowed this group of animals to live and reproduce independently of the aquatic environment [1,2]. The determining innovation that facilitated these amniotes to colonize diverse terrestrial ecosystems was the cleidoic egg, considered one of the most outstanding evolutionary events in the history of vertebrates [3,4].

The eggshell is a multifunctional physiological barrier that ensures embryonic development and survival [5], regulates gas and water exchange between the egg and the nest [6], and provides a calcium reservoir for the growing embryo [7]. It is an example of the perfect organic-inorganic combination that yields materials with extraordinary attributes of flexibility and toughness. The organic components are essentially protein- and sugar-based polymers [8,9], while among the biominerals are hydroxyapatite, calcium carbonate in the form of calcite or aragonite, and silicon dioxide [10,11]. Structural proteins can be further divided into those dominated by regions of rigid secondary structure (such as the triple helix in collagen and the α-helix and β-sheet in keratin) and those containing mostly amorphous and random-coil domains (as in elastin, resilin, and abductin) [12,13]. The physical-chemical and mechanical properties conferred by these organic

Corresponding author
e mail: maria.alvarez@fbqf.unt.edu.ar (Rosa María Susana Álvarez)

components to the eggshell led collagen and keratin to emerge as new sustainable biomaterials because of their easy availability, biodegradability, and inherent biocompatibility between cells and tissues [14,15].

Reptile eggshells are usually classified as "hard" or "soft" and/or "flexible" [16], although their structural conformation and water requirements exhibit a varying spectrum [17]. In this regard, research focuses especially on the general conformation of the shell and on the mechanisms that promote its mineralization [18,19], while limited information on the structural characterization, compositional analysis, and mechanical properties of the biomaterials in the eggshell of this group of vertebrates is available.

Tegu (Squamata: Teiidae) of the genus Salvator is one of the largest South American lizards and is recognized in the international live animal trade and commercially exploited for the qualities of its skin [20]. The Black and White Tegu, Salvator merianae, is the southernmost lizard of the genus and is distributed over a large fraction of Argentina [20,21]. Its annual oviposition ranges from 20 to 50 eggs of whitish color and oval shape, with a soft and resistant but permeable to water shell [22]. Recently, using optical microscopy, scanning electron microscopy, energy-dispersive X-ray spectroscopy, and Raman spectroscopy it was demonstrated that the eggshell of Salvator merianae has an organic and inorganic composition, notably different from that described for reptile eggshells [23]. For the first time, mucopolysaccharides were identified in the surface layer of a reptile egg, as well as hydroxyapatite in the deep section of the shell. The presence of this biomineral is remarkable as it contradicts generalizations that assume calcium carbonate as the only mineral source in the eggs of this group of vertebrates [16,24]. On the other hand, ultrastructural analysis evidenced two morphologically different types of fibers. Indeed, 85% of the thickness of the shell consists of a dense mesh of parallel fibers, distinguished by the presence of intrafibrillar alveoli. The remaining 15% of the shell consists of two sheets of compact fibers exhibiting plywood stacking structure [23].

The morphological peculiarities of the Salvator merianae egg and its evident ability to adapt to the development of the embryo, motivate to deepen the study of the molecular nature of the fibrillar components of its shell with a double purpose: (i) From developmental biology, understanding the structural and molecular conformation of the shell of Argentine Black and White Tegu would provide new insights into reproductive strategies in these sauropsids. Specifically, knowing the structural elements of the shell and their behavior will make it possible to establish parameters for the development of artificial incubation technologies. The artificial incubation of Salvator merianae eggs and the zootechnical management of animals born in captivity are substantial for the sustainable use of this species with a more visible impact on its conservation [22]. (ii) Due to the great interest that currently exists in the investigation of fibrillar biopolymers because of their great functionality and their natural abundance, determining the biomaterials that make up the Salvator merianae eggshell will allow to advance in the knowledge of these macromolecules in the field of biomaterial engineering. In particular, fibrillar biopolymers have attracted interest for their behavior as elastomeric materials or as hydrogel systems [25].

In the present work, we analyzed by Raman microscopy the molecular fingerprint of the fibrillar polymers of the eggshell of the Argentine Black and White Tegu. Raman spectroscopy has proven to be a powerful analytical technique in the study of biological materials, providing robust correlations between spectral information and the biochemical and structural nature of the biomaterials that comprise them. In addition, we complement the spectroscopic study with transmission electron microscopy and with brightfield and polarized light optical microscopy to determine the fibrillar morphology and its spatial distribution.

2 Materials and Methods

2.1 Biological material

To exclude possible modifications in the structure and chemical composition of the shells associated with incubation or embryonic development, recently oviposited eggs (up to 12 h after laying) in a perfect

state of preservation were used. Eggs (n =12) were taken from six nests built by Salvator merianae females (with at least two previous clutches). The mean weight of the females was 4 kg, and average snout-vent length >35 cm. The animals were housed at the Experimental Lizard Hatchery of the Facultad de Agronomía y Zootecnia of the Universidad Nacional de Tucumán, located at Finca "El Manantial" (26º51´S, 65º17´W), province of Tucumán, Argentina. Animal handling and care protocols were carried out by the "Guide for the care and use of laboratory animals" [26]. All experiments have been examined and approved by the Ethics Committee of Consejo de Investigaciones de Universidad Nacional de Tucumán (CIUNT).

2.2 Transmission Electron Microscopy (*TEM*)

Small pieces of eggshells (n = 6) were fixed in Karnovsky's fixative [27] at half concentration for 24 h at 4-5 °C, post-fixed with 2% Osmium tetroxide (Ted Pella, California, U.S.A), dehydrated in increasing concentrations of acetone and embedded in Spurr resin (Ted Pella, California, U.S.A). Ultrasections were counterstained with 2% Uranyl acetate (Ted Pella, California, U.S.A) and observed with Zeiss Libra 120 transmission electron microscope (Carl Zeiss, Oberkochen, Germany) controlled with WinTEM user interface and system software (Carl Zeiss).

2.3 Light microscopy

For histological studies, 6 whole eggs were fixed in a 4% phosphate-buffered formaldehyde solution at pH 6.8 [28] for 12 h at 4°C. Small pieces of shell from each egg (n = 12) were dehydrated in ethyl alcohol, diaphanized in xylene, embedded in paraffin-celloidin and serially sectioned at 8 µm. For the determination of collagen fibers the sections were stained for 30 min with Sirius red (0.1% of Sirius red F3B; Sigma-Aldrich Co., St Louis, MO, United State in saturated aqueous picric acid), as described by Junqueira *et al* [29] for collagen bundle staining. In addition, the spatial distribution between keratin and collagen was analyzed by Heidenhain's Azan staining [30]. Sections stained with Sirius red and Heidenhain's Azan were analyzed with an Olympus BX51 brightfield and polarized light microscope (Olympus Corporation, Tokyo, Japan) equipped with an Olympus Q Color 5 digital camera controlled with Pro Express 6.0 software (Media Cybernetics, Rockville, Illinois, USA).

2.4 Raman microscopy

Square fractions (3mm×3mm approx.) of the *Salvator merianae* eggshell were mounted on a gold-coated slide suitable for Raman microscopy. Raman measurements, between 3500 and 50 cm^{-1}, were performed with a DXR confocal Raman Microscope (Thermo Fisher Scientific, U.S.A.) equipped with a motorized stage with 3 µm of spatial resolution (x, y axes) and 2 µm of confocal depth resolution. A diode-pump solid-state laser of 780 nm (5 cm^{-1} spectral resolution) was focused on the sample with a 20× objective. For data collection, excitation at 24 mW of power and a confocal aperture of 50 µm slit were used. The spectroscopy examination of the cross-section of each eggshell piece was carried out at 7 different depth levels, approximately 25-40 micrometers apart. The spectra were collected from three different sampling points, located at each depth level, obtaining a total of 21 spectra from each sample. Each sampling point yielded one individual spectrum, which was acquired by accumulating 60 expositions with an exposure time of 3 seconds each. Three samples of eggshells were used, belonging to three different specimens.

Reference spectra of collagen (I/II), elastin/collagen III and β-keratin were acquired from tendon, aorta, and claw samples, respectively, taken from different specimens of *Salvator merianae*, which had already been euthanized in the framework of other studies. For euthanasia, the animals were first anesthetized with diazepam (2.5 mg/kg) and intramuscular ketamine (25 mg/kg) and then supplied with intracardiac injections of sodium pentobarbital (100 mg/kg) [31]. The α-keratin reference spectrum was acquired from a human nail sample. The water reference spectrum was obtained from a 20 µL drop of tri-distilled water. All reference spectra were recorded following similar conditions as for eggshell spectra in terms of excitation energy and spectral accumulation. Spectroscopic experiments were carried out at room temperature.

2.5 Data analysis

Spectral data were processed with the OMNIC 8 Software suite (Thermo Scientific, U.S.A). All the spectra (n = 63) were individually baseline corrected using a linear algorithm and then smoothed with 13 data point with the Savitzky-Golay algorithm [32]. Subsequently, to minimize slight spectral differences that may arise between the three sampling points at a given depth in an eggshell sample, a single average-spectrum was obtained for each depth (n = 7 per eggshell sample). The spectral analyzes were carried out on the average-spectra, going from #1 at the outer surface to the #7 at the inner one in a given eggshell sample.

The OMNIC Specta software (Thermo Scientific, U.S.A) is a task-based tool for processing, searching, and interpreting Raman spectra. The multi-component search tool of this software was used to look for the mathematical combinations involving the reference spectra that best describe the spectra taken from the eggshell at different depths. The library with the reference spectra, constructed specifically for this purpose (see above), also included the spectrum of L-cystine (crystalline, 98%) extracted from a commercial spectra library (Thermo Scientific) and the spectrum of the zona pellucida (ZP) of bovine oocytes that was used as reference of glycoproteins [33]. Since the algorithm allows the maximum number of components to be 4, the results were used as illustrative with respect to the principal components that contribute to a specific spectrum.

3 Result and Discussion

Micrographs of radial sections of *Salvator merianae* eggshell are presented in Fig 1. Ultrastructural analysis revealed the fine structure of the fibers and matrix. The outer surface consists mainly of an amorphous material exhibiting zones with varying degrees of electrodensity, Fig 1(a). The intermediate region of the shell is composed of fibers characterized by the presence of alveoli inside, Fig 1(b). The interfibrillar matrix exhibits a granular appearance, as can be seen in Fig 1 (c), and contains clusters of dispersed osmophilic fibrils, which are shown in Fig 1(d). In the deep zone of the shell, the compact fibers are characterized by their orthogonal organization. A high electrodensity sheath between the fibers is noticeable, Fig 1(e).

Picrosirius Red staining (also called PSR or "Sirius red" staining) is a selective staining suitable for studying and quantifying the collagen lattice in the extracellular matrix [34], with the same specificity properties as with the immunohistochemical technique [35]. Heidenhain's Azan staining was used for the selective demonstration of cells and components of the extracellular matrix [30]. Images of Salvator merianae shell sections stained with Sirius red and Heidenhain's Azan are presented in Fig 2. Radial shell sections stained with Sirius Red exhibited mainly long wavelength polarization colors: yellow-orange to red results suggest a dominance of type I and II collagen fibers [36]; type III collagen exhibited a faint greenish birefringence [37] adjacent to the section near the plaques and fissures of the shell surface, Fig 2 (a). Shell sections stained with Heidenhain's Azan exhibited an intense red color, characteristic of keratins. Although, this coloration is present throughout the entire thickness of the shell, it manifested a tintorial dominance in the middle and upper zones. In addition, this trichrome staining also revealed blue-colored collagen fibers mixed with keratin fibers, Fig 2 (b).

The Raman spectra of the recently oviposited eggshell of *Salvator merianae* were acquired from seven sampling points located at different depths from the outer surface until the inner surface. A detailed comparison was made between all the spectra to look for differences reflecting the distribution of bio-components along the eggshell cross-section; a single spectral profile, representative of the global composition of the system, was obtained by averaging the seven spectra. Figure 3 compares the representative-spectrum of the eggshell, with reference spectra for collagen (types I, II), keratin with a high proportion of β-sheet/random coil conformations, and α-helix-rich keratin. The spectra of L-cystine to mimic the contributions from the presumed amorphous matrix rich in disulfide bonds and of liquid water are also shown in Fig 3.

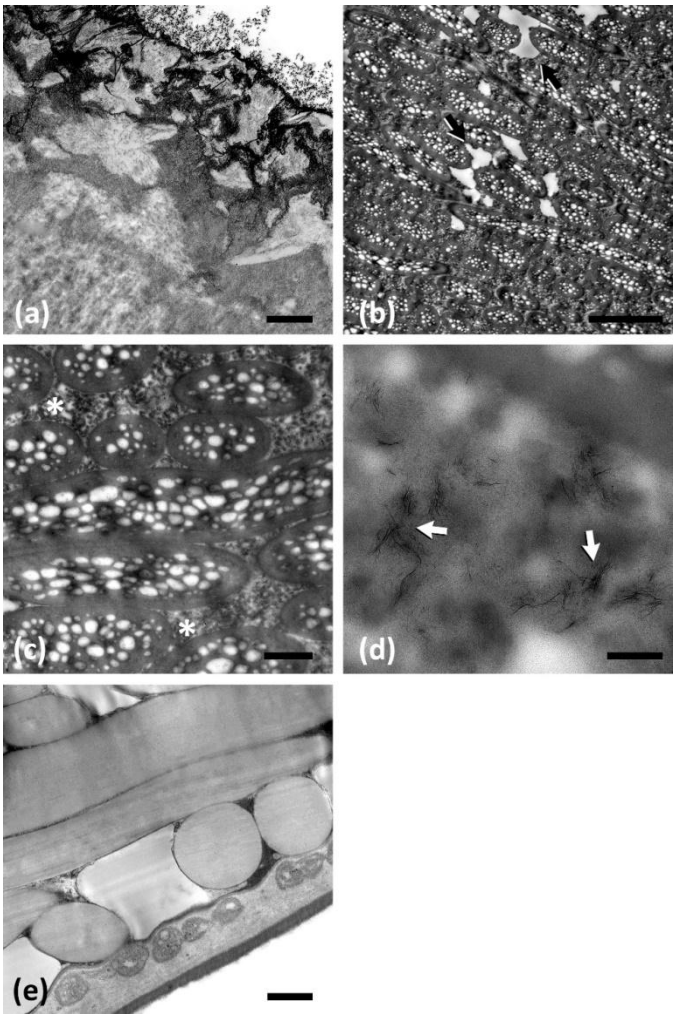

Fig 1. Transmission electron microscopy (TEM) photographs of Argentine Black and White Tegu (*Salvator merianae*) eggshells: (a) Radial section showing the amorphous conformation of the shell surface. Note the amorphous nature of the matrix along with moderate to intense electrodensity zones. Scale bar 1µm. (b) Alveolar fibers of the middle and upper zone of the shell. Arrows point to wide interfibrillar spaces. Scale bar 5µm. (c) Detail of the alveolar fibers of the deep zone of the shell. The asterisks indicate the granular interfibrillar material. Scale bar 1 µm. (d) Detail of the microfibrils between the alveolar fibers. Scale bar 200 nm. (e) Radial section showing compact fibers arranged in a double layer, sectioned longitudinally and transversely. Scale bar 1µm. In all images outside of the eggshell is up.

Based on the morphological/structural information derived from transmission electron microscopy and the stain assays, as well as from related literature, the Raman spectral analysis was carried out on the premise that the main bio-components of *Salvator merianae* eggshell are collagen and keratin, both embedded in an amorphous sulfur matrix-forming cystine-like disulfide bonds. Sexton *et al* [38] studied the amino acids eggshell, with reference spectra for collagen (types I, II), keratin with a high proportion of the β-sheet/ random composition in eggshells of several squamate reptiles and found that flexible eggshells contain significantly high levels of proline; proline, together with hydroxyproline and glycine constitute the collagen, the biopolymer that confers flexibility to the soft eggs [39]. In addition, it was demonstrated that theflexible

eggshell of Taiwan cobra snake (Naja atra) is composed of a wavy and random arrangement of keratin fibers as well as collagen layers, being keratin the main protein constituent of that system. Moreover, it was reported that the α-helix, β-sheet, and β-turn fractions of keratin extracted from snake eggshell were 64.2%, 13.8%, and 22.0%, respectively according to the ATR-FTIR deconvolved amide I (AmI) band [39]. On the other hand, previous studies on the *Salvator merianae* eggshell by energy-dispersive X-ray spectroscopy evidenced high sulfur content well distributed throughout the cross section of the shell [23]. Those results provide the basis for assuming the existence of a sulfur matrix in this system; it can be related to a previous study that reported the identification of a new protein rich in cysteine, found in the membranes of the eggshells of birds and some lizards [40]. By reductive alkylation of avian eggshell membranes followed by proteolytic digestion, the cysteine-rich protein was characterized as possessing a modular sequence architecture that is formed from multiple disulfide-containing units in a C-X4-C-X5-C-X8-C-X6-C-X4-C-X5-C-X8-C-X11 amino acids repetitive pattern, where X represents any amino acid, except cysteine [40]. Raman spectral signals from other macromolecules like elastin and glycosaminoglycans are also expected to be observed. Studies of the three-dimensional organization of fibrils in tissues have shown that these are embedded in a viscous proteoglycan matrix [41], which is considered to play an important role in the mechanical strength of the fibers [42].

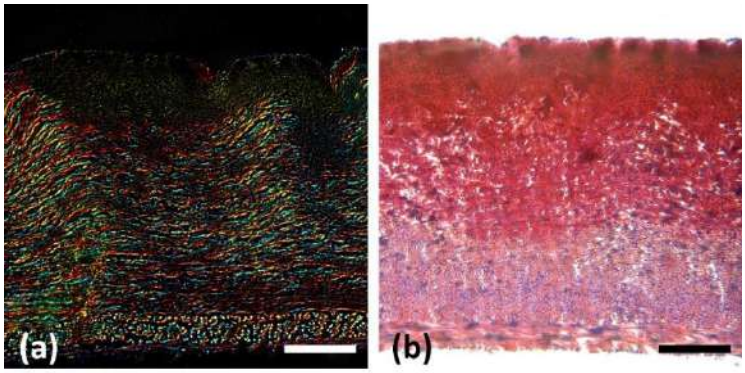

Fig 2. Light microscopy micrographs of Salvator merianae eggshells. (a) Polarized light micrograph of a cross-section eggshell stained with Sirius red. Scale bar 40 μm. (b) Light micrograph of a cross-section eggshell stained with Heidenhain's Azan. Note the intense red coloration of the keratin fibers. Scale bar 37 μm. In both images outside of eggshell is up.

Bands from the complex protein domain are easily detected in the eggshell, representative-spectrum is shown in Fig 3: i) the amide I (AmI) and amide III (AmIII) modes, appearing in the intervals between 1700-1620 cm^{-1} and 1280-1210 cm^{-1}, respectively; ii) several vibrations of aromatic amino acids; iii) the CH_2/CH_3 bending mode of the peptide backbone, located at 1448 cm^{-1} [43]. One of the interesting characteristics of the eggshell spectrum is the strong band at 499 cm^{-1}, which is associated with disulfide bonds, characteristic of certain fibrillar proteins [40,43-45]. Most of the bands observed in the *Salvator merianae* eggshell representative-spectrum, together with their tentative assignments are presented in Table 1.

Due to the fibrillar nature of collagen, as well as the abundance of collagen-specific amino acids like hydroxyproline, the Raman spectrum of this macromolecule is unique and can easily be discriminated from most other proteins [46]. Thus, in the spectrum of the *Salvator merianae* tendon (Fig 3), the wavenumbers of the AmI band (1665 cm^{-1}) and the AmIII component at 1266 cm^{-1} are consistent with the high proportion of α-helix conformations that characterizes the structure of collagen (typesI/ II) [46,47]; the less abundant β-sheet/random conformations of collagen are associated to the shoulders around 1678 and 1637 cm^{-1}(Am I) and to the strong band 1245 cm^{-1} (AmIII) [48,49]. Other typical collagen features are observed at 1097 cm^{-1}, assigned to the NCH deformation of proline [50], at 932 and 917 cm^{-1}, corresponding to the C-C

stretching mode of the backbone formed by the known Gly-X-Y sequences and to the proline ring vibration, respectively [49], and 873 cm^{-1}, a signal that arises from the hydroxyproline ring vibration [49]. All these collagen bands are clearly manifested in the representative spectrum of the eggshell, as is highlighted in Fig 3. Similarly, there are also several bands in the spectrum of the eggshell that can be confidently associated with the vibrations of the keratin molecules. It is even possible to discriminate between specific bands of keratin rich in α-helix conformations from those with predominant β-sheet or disordered structures. Thus, although the component of AmI at 1665 cm^{-1} and that of AmIII at 1245 cm^{-1} can be ambiguously assigned to β-keratin vibrations, the features located at 1611, 1554, 1201, 1186, 1002, 760, and 642 cm^{-1}, all of them attributable to vibrations of aromatic amino acids [44,51] (see Table 1), show very good correlation both in position and in relative intensities with the spectral profile of the reference β-keratin. In turn, the more ordered structure of α-keratin chains is manifested in an AmI component located at 1651 cm^{-1} in the spectra of the eggshell, in very good agreement with the reference spectrum and with literature data [48,51,52]; other features are observed at 1315 cm^{-1} (Cα-H bending mode) and 934 cm^{-1} (skeletal C-C stretch αhelix). The strong and asymmetric band at 500 cm^{-1} in the spectra of the eggshell is assigned to the stretching mode of various disulfide bonds. The typical location in keratin (whether α or β) is at ~ 510 cm^{-1} and corresponds to the most stable gauche-gauche-gauche (ggg) conformation around the S-S bond [44,52]; in the spectra of the eggshell, this contribution is observed as a shoulder at ~ 509 cm^{-1}. Other less stable arrangements around the SS link, defined as trans-gauche-trans (tgt) (540 cm^{-1}) and gauche-gauche-trans (ggt) (525 cm^{-1}) could be integrating the wide shoulder of the main band, while the maximum at 499 cm^{-1} is interpreted to be originated in disordered conformations similar to those observed for cystine dimer [52].

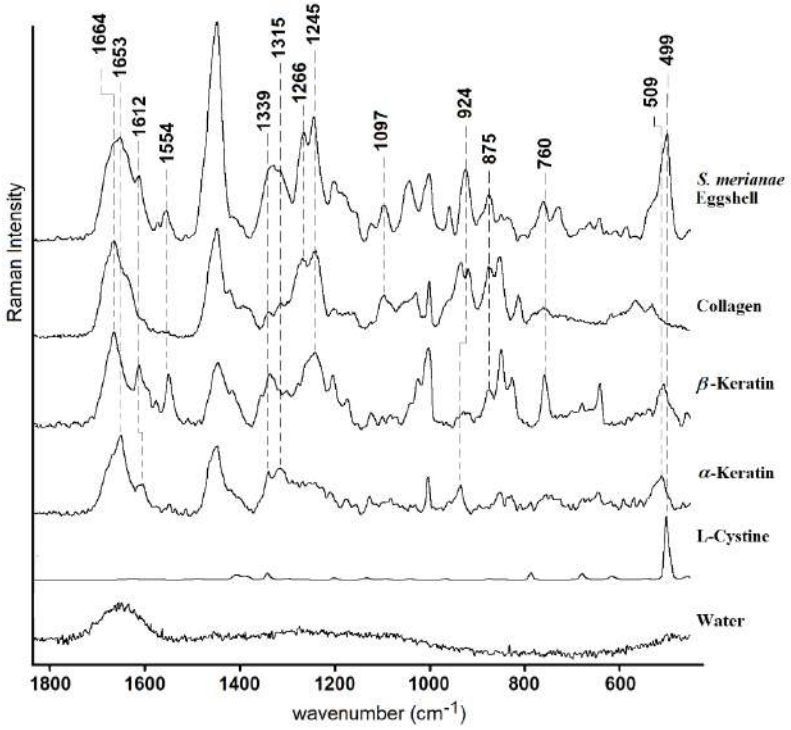

Fig 3. Comparison between the representative-spectrum of the *Salvator merianae* eggshell and the spectra of collagen (types I/II, from Salvator merianae tendon), β-keratin (from *Salvator merianae* claw), α-keratin (from a human nail), L-cysteine (solid) and liquid water, taken as references to identify their contribution to the average spectrum.

Table 1. Wavenumbers (cm^{-1}), relative intensities, and tentative assignment of most of the bands observed in the 1800–450 cm^{-1} region of the representative-spectrum of the Salvator merianae eggshell.

Wavenumber[a] (cm^{-1})		Assignment	References
1664	sh	Amide I (collagen; β-keratin)	[48,53]
1653	s	Amide I (α-keratin)	[48]
1612	m	Tyr (keratin)	[44,52]
1554	m	Trp (keratin)	[44,52]
1448	vs	CH_3/CH_2 def. (collagen; keratin)	[33,53]
1330	s	CH_2 scissoring def. (Keratin)	[33,46,53]
1315	sh	Cα-H def. (α-keratin)	[44,46]
1266	s	Amide III α-helix (collagen)	[48,49]
1245	s	Amide III β-sheet/random coil (collagen; β-keratin)	[44,48,49,52]
1201	m	Tyr; Phe (β-keratin)	[44]
1186	sh	Tyr (keratin)	[44,52]
1097	m	NCH def. Pro; C-O stretch. carbohydrate (collagen)	[34,50]
1042	m	S-O stretch. sulfonate; C-O stretch. carbohydrate (β-keratin; collagen)	[44]
1002	m	Phe (collagen; keratin)	[49,33]
958	m	$–PO_4^{-3}$ stretch. (Hydroxyapatite)	[23]
924	s	C-C stretch. Pro/Hypro ring; C-C stretch. α-helix; $C\text{-}COO^-$ (collagen; α-keratin)	[44,46,49,50]
875	m	C-C stretch. Pro/Hypro ring (collagen)	[49]
847	w	C-C stretch. Pro/Hypro ring; Tyr (collagen; keratin)	[44,46,49,52]
760	m	COO^- def.; Trp (collagen; β-keratin)	[50,52]
728	m	C-S stretch. (collagen)	[45,49]
662	w	C-S stretch. cys (keratin)	[44]
640	w	C-S stretch. ; Tyr (keratin)	[44,52]
584	w	C-S stretch. (keratin)	[45,52]
530	sh	S-S stretch. (tgt) (collagen)	[49]
509	sh	S-S stretch. (ggg) (keratin)	[44,52]
499	s	S-S stretch. cys (keratin; cystine-rich unordered matrix)	[45,52]

[a] vs: very strong; s: strong; m: medium; w: weak; sh: shoulder. [b] Phe.: phenylalanine; Tyr.: tyrosine; Trp.: tryptophan; cys.: cystine; stretch.: stretching; def.: deformation.

The CH_2/CH_3 bending band (1448 cm^{-1}) is known to be insensitive to protein secondary structure and only to depend on the total concentrations of methyl and methylene groups [53]. Then, its intensity is used to evaluate the variability of the main bands throughout the eggshell radial section. In Fig 4, the seven spectra (#1 to #7) acquired from a single eggshell are shown as overlapped. The radial view of the eggshell with the positions of the sampling points located at depths of ~10, 35, 60, 85, 115, 145, and 185 μm is included. As can be seen, the most noticeable difference between the spectra is the progressive decrease of the AmI band going from sampling point #1 to #5. The intensity ratio I_{1653} / I_{1448} in spectra #2, #3, #4, and #5 are estimated to be 11%, 27%, 36%, and 42%, respectively, lower than in spectrum #1; in spectra #6 and #7 the intensity ratio remains constant and the same as in #5. Similar behavior is observed for the bands at 1613

cm^{-1} (Tyr). The same trend, though to a lesser extent, is shown by the signals at 1002, 924, 875, 761, and 499 cm^{-1}, while the remaining protein bands present negligible intensity changes (Fig 4). Relevant intensity variations are graphically represented in Fig 5. Particularly striking is the fact that the bands corresponding to the AmIII mode do not show significant differences either in relative intensities or in shifts when the different spectra are compared, (Fig 5(b)). This leads us to think that the pronounced intensity change of the spectral profile in the 1700-1600 cm^{-1} interval is due, in part, to the contribution of the OH bending mode of liquid water. It has been demonstrated that liquid water is an active component to be taken into account when characterizing skin constituents by applying a biophysical model; water played an important role in fitting the broad Raman band at 1645 cm^{-1} [48,54].

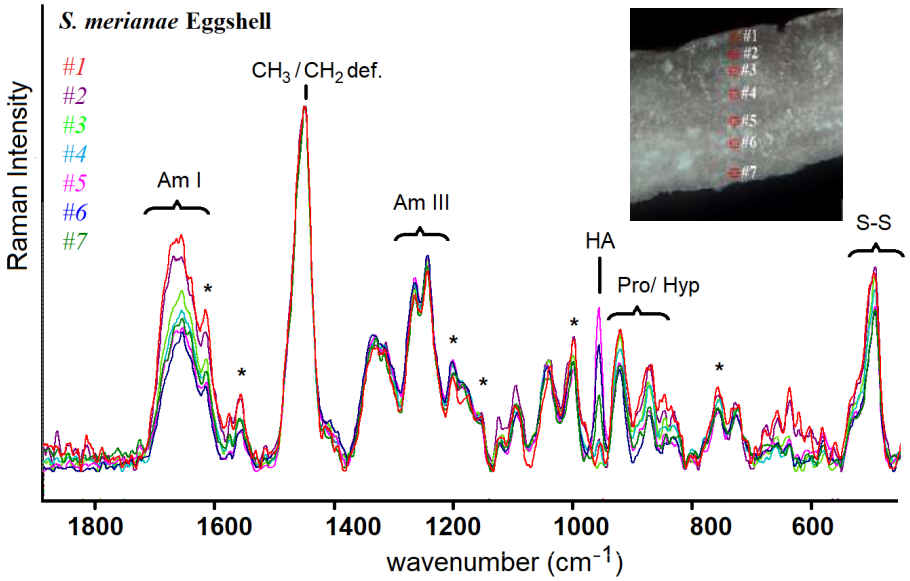

Fig 4. Raman average-spectra acquired at different depths in the radial section of the eggshell of the Argentine Black and White Tegu. The spectral region comprised between 1800 and 450 cm^{-1} is shown. The spectra are normalized with the CH_2/CH_3 bending mode at 1448 cm^{-1}. The main bands associated with characteristic protein vibrations together with the peak assigned to the PO_4^{3-} symmetrical stretch of hydroxyapatite (HA) are identified. Bands associated with aromatic amino acid vibrations are denoted with *. Inset: Microphotography of a radial section of the eggshell indicating the seven sampling points that originate the spectra #1 to #7. Outside of eggshell is up.

The spectral contribution from liquid water, mainly to the spectra of the outer layers of the eggshell is supported by the micrograph acquired by transmission electron microscopy from the alveolar fibers of the interzone, where large inter-fibrillar spaces are observed (see Fig 1(b)). It can be hypothesized that such inter-fibrillar spaces are related to the water interchange between embryo and nest and could provide thermal protection against abrupt temperature changes during incubation [55,56]. The sharp peak observed at 958 cm^{-1}, assigned to the symmetric PO_4^{3-} stretch of hydroxyapatite, also shows drastic intensity variation among the different sampling points; its maximum spectral contribution is observed in spectrum #5 and decreases going to #6 and #7 (Fig 4). This behavior is in good correlation with the location of the calcium/ phosphorous deposits, previously determined by energy-dispersive X-ray spectroscopy [23].

The apparent constant decrease observed in the intensities of some specific bands attributed to the main bio-components while others are almost invariant, does not allow conclusions to be drawn from the direct spectral comparison regarding their distribution at different levels of eggshell depths (Fig 4).

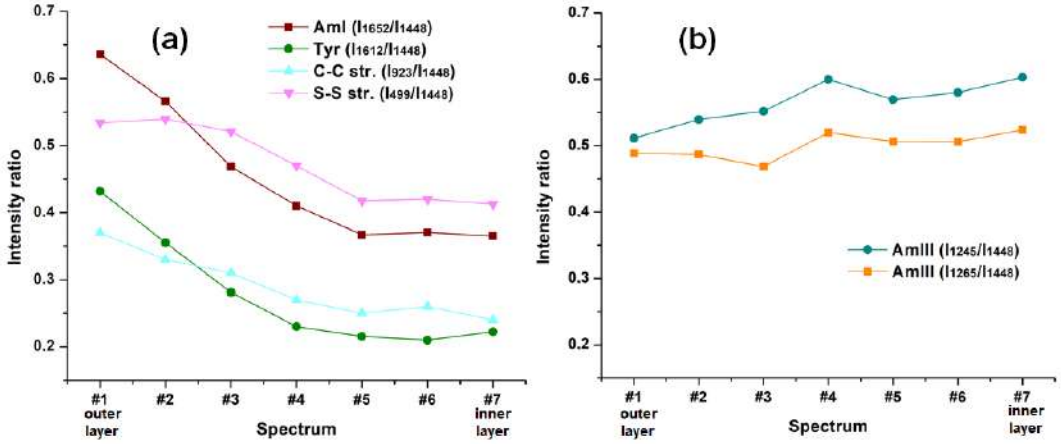

Fig 5. Intensity ratio variation of specific bands as a function of the seven sampling points in the eggshell cross section (see inset of Fig 4). (a) Intensity ratios of the 1652, 1612, 923, and 509 cm^{-1} bands with respect to the band at 1448 cm^{-1}. (b) Intensity ratios of 1265 and 1245 cm^{-1} bands with respect to the band at 1448 cm^{-1}.

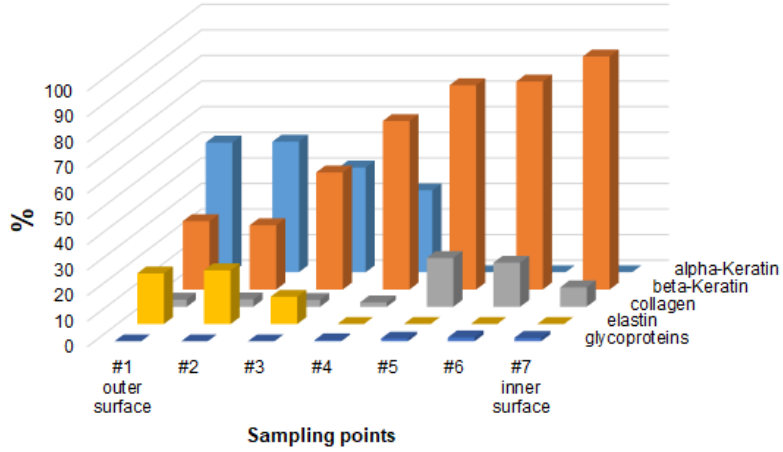

Fig 6. Estimated relative biomolecular composition (%) at each of the seven sampling points of the eggshell cross section.

A multiple component analysis was performed for each of the seven spectra of the eggshell. This analysis consists of the search for the best combination of (four) bio-components that generate a composite spectrum that matches a problem spectrum, using a specific tool for this purpose provided by the OMNIC Specta software. Apart from the reference spectra presented in Fig 3, those corresponding to a sample rich in elastin (taken from a Salvator merianae aorta sample) and to one of unidentified glycoproteins (extracted from the zona pellucida of gametes mammalian) [33] were also taken into account for the multi-component analysis. Figure 6 depicts the estimated relative contributions from different bio-components to the best four-component composite found for each spectrum of the eggshell. The results obtained by this approach indicate that the dominant component at all levels of the eggshell is keratin. Collagen I/II, also present in all spectra, is predicted to a much lesser extent in terms of abundance. Interestingly, the estimated composite spectra for the outermost layers of the eggshell show a high structural complexity since, apart from keratin in different conformations, a relatively high proportion of elastin/collagen III is included. In the innermost layers, the

contributions of α-keratin and elastin are neglected, so that the organic composition in this region of the shell is predicted almost exclusively composed of β-keratin; a slight contribution from the glycoprotein spectrum, which is interpreted as a manifestation of the carbohydrate component, was also detected by this spectral analysis method. These assessments, although approximate, show a good concordance with the eggshell morphology, determined by transmission electron microscopy.

The interaction between collagen and keratin has been shown to have a high potential in the creation of composites with biomedical applications; for instance, polymeric membranes have been developed using both biomaterials as support for epithelial cells culture [57]. In concordance, the evidence of the ubiquity of both collagen and keratin (Fig 2) and of their dominant contributions to the spectral profile at each sampling point presented here (Fig 6) allow us to glimpse the inherent capacity of the eggshell of this reptile in the field of biomaterials.

4 Conclusions

This is the first study to characterize the organic components that make up the eggshell of Salvator merianae. The structural analysis performed by different microscopy techniques reveals an interesting fibrillar organization, consisting mainly of collagen of different types and keratins with the two major folds well defined. A gradual change in the relative content between these components is observed at different depth levels of the eggshell cross-section by Raman microscopy.

The results presented here open new questions related to the extraordinary sulfur concentration detected throughout the thickness of the eggshell while laying the foundation for further studies aimed at elucidating the mechanisms that regulate the physicochemical properties of the eggshell as the embryo develops.

In-depth knowledge of the characteristics and functioning of the major organic components in this complex system opens expectations related to the development of new materials.

Acknowledgments

This paper has been partially funded by PIUNT Project 26/A605 to the Secretaría de Ciencia, Arte e Innovación Tecnológica (SCAIT) of the Universidad Nacional de Tucumán. We also thank the technicians Juan Oliver and Roque Carranza for their help in the field work. A.N.D. is grateful to CONICET for his Doctoral fellowship. R M S A. is career researcher of CONICET.

References

1. Reisz R R, The Origin and Early Evolutionary History of Amniotes, *Trends Ecol Evol*, 12(1997)218–222.
2. Blackburn D G, Stewart J R, Morphological Research on Amniote Eggs and Embryos: An Introduction and Historical Retrospective, *J Morphol*, 282(2021)1024–1046.
3. Sander P M, Reproduction in Early Amniotes, *Science*, 337(2012)806–808.
4. Starck J M, Stewart J R, Blackburn D G, Phylogeny and Evolutionary History of the Amniote Egg, *J Morphol*, 282(2021)1080–1122.
5. Hallmann K, Griebeler E M, Eggshell Types and Their Evolutionary Correlation with Life-History Strategies in Squamates, PLoS One, 10(2015)e0138785; doi.org/10.1371/journal.pone.0138785
6. Tang W, Zhao B, Chen Y, Du W, Reduced Egg Shell Permeability Affects Embryonic Development and Hatchling Traits in Lycodon rufozonatum and Pelodiscus sinensis, *Integr Zool*, 13(2018)58–69.
7. Jee J, Mohapatra B K, Dutta S K, Sahoo G, Sources of Calcium for the Agamid Lizard Psammophilus blanfordanus During Embryonic Development, *Acta Herpetol*, 11(2016)171–178.
8. Gough C R, Rivera-Galletti A, Cowan D A, Salas-De La Cruz D, Hu X, Protein and Polysaccharide-Based Fiber Materials Generated From Ionic Liquids: A Review, *Molecules*, 25(2020)3362; doi.org/10.3390/molecules25153362.

9. Souza P R, de Oliveira A C, Vilsinski B H, Kipper M J, Martins A F, Polysaccharide-Based Materials Created by Physical Processes: From Preparation to Biomedical Applications, *Pharmaceutics*, 13(2021)621; doi.org/10.3390/pharmaceutics13050621.
10. Pančić M, Torres R R, Almeda R, Kiørboe T, Silicified Cell Walls as a Defensive Trait in Diatoms, *Proc Royal Soc: Biol Sci*, 286(2019)20190184; doi. org/10.1098/rspb.2019.0184.
11. Le Roy N, Stapane L, Gautron J, Hincke M T, Evolution of the Avian Eggshell Biomineralization Protein Toolkit - New Insights From Multi-Omics, *Front Genet*, (2021)672433; doi.org/10.3389/fgene.2021.672433.
12. Chen P Y, McKittrick J, Meyers M A, Biological Materials: Functional Adaptations and Bioinspired Designs, *Prog Mater Sci*, 57(2012)1492–1704.
13. Rauscher S, Pomès R, Structural Disorder and Protein Elasticity. In: Fuxreiter M, Tompa P, (eds). Fuzziness. Advances in Experimental Medicine and Biology, (Springer, New York, NY) 2012, p.159-183.
14. Shavandi A, Silva,T H, Bekhit A A, Bekhit A E-D A, Keratin: Dissolution, Extraction and Biomedical Application. *Biomater Sci*, 5(2017)1699–1735.
15. Sorushanova A, Delgado L M, Wu Z, Shologu N, Kshirsagar A, Raghunath R. Mullen A M, Bayon Y, Pandit A, Raghunath M, Zeugolis D I, The Collagen Suprafamily: from Biosynthesis to Advanced Biomaterial Development, *Adv Mater*, 31(2018)1801651; doi.org/10.1002/adma.201801651.
16. Packard G C, Packard M J, Evolution of the Cleidoic Egg Among Reptilian Antecedents of Birds, *Am Zool*, 20(1980)351–362.
17. Packard M J, DeMarco V G (1991). Eggshell structure and formation in eggs of oviparous reptiles. In: D. C. Deeming & M. W. J. Ferguson (Eds.), Egg incubation: Its effects on embryonic development in birds and reptiles. (Cambridge University Press) 1991, p. 53–69.
18. Makkar S, Liyanage R, Kannan L, Packialakshmi B, Lay J O (Jr), Rath N C, Chicken Egg Shell Membrane Associated Proteins and Peptides, *J Agric Food Chem*, 63(2015)9888–9898.
19. Hallmann K, Griebeler E, Eggshell Types and Their Evolutionary Correlation with Life-History Strategies in Squamates, *PLoS One*, 10(2015); doi.org/10.1371/journal.pone.0138785.
20. Jarnevich C S, Hayes M A, Fitzgerald L A, Yackel Adams A A, Falk B G, Collier M A M, Bonewell L R, Klug P Naretto E S, Reed R N, Modeling the Distributions of Tegu Lizards in Native and Potential Invasive Ranges, *Sci Rep*, 8(2018)10193; doi.org/10.1038/s41598-018- 28468-w.
21. Murphy J C, Jowers M J, Lehtinen R M, Charles S P, Colli G R, Peres A K (Jr), Hendry C R, Pyron R A, Cryptic, sympatric diversity in tegu lizards of the Tupinambis teguixin group (Squamata, Sauria, Teiidae) and the description of three new species, *PLoS One*, 11(2016)1–30.
22. Manes M E, Principles for the Productive Breeding of Tegu Lizards. Bilingual Spanish-English Edition. Facultad de Agronomía y Zootecnia, Universidad Nacional de Tucumán, Tucumán, Argentina. 2016
23. Campos-Casal F H, Cortez F A, Gomez E I, Chamut S N, Chemical Composition and Microstructure of Recently Oviposited Eggshells of Salvator merianae (Squamata: Teiidae), *Herpetol Conserv Biol*, 15 (2020)25–40.
24. Choi S, Han S, Kim N H, Lee Y N, A Comparative Study of Eggshells of Gekkota With Morphological, Chemical Compositional and Crystallographic Approaches and its Evolutionary Implications. *PloS One*, 13(2018)1–31.
25. Goor O J G M, Hendrikse S I S, Dankers P Y W, Meijer E W. From Supramolecular Polymers to Multi-Component Biomaterials, *Chem Soc Rev*, 46(2017)6621–6637.
26. Committee for the Update of the Guide for the Care and Use of Laboratory Animals. 8th edn, National Academy of Sciences, USA, 2011.
27. Karnovsky M J, A Formaldehyde-Glutaraldehyde Fixative of High Osmolality For Use in Electron Microscopy, *J Cell Biol*, 27(1965)137–138A.
28. Suvarna K, Layton C, Bancroft J D, Bancroft's Theory and Practice of Histological Techniques. 7th edn. Churchill Livingstone Elsevier, (eds). London, UK, 2008.
29. Junqueira L C U U, Bignolas G, Brentani R R, Picrosirius Staining Plus Polarization Microscopy, a Specific Method for Collagen Detection in Tissue Sections, *Histochem J*, 11(1979)447–455.
30. Martoja R, Martoja PM, Técnicas de Histología Animal. 1ra Edición. Toray-Masson, (eds) Barcelona, España.1970.

31. Baer C K, Guidelines on euthanasia of nondomestic animals. Yulee Fla, American Association of Zoo Veterinarians (eds). Florida, USA. 2006, p. 111.
32. Savitzky A, Golay M J E, Smoothing and Differentiation of Data by Simplified Least Squares Procedures, *Anal Chem*, 36(1964)1627–1639.
33. Rizo G, Roldán-Olarte M, Miceli D C, Jiménez L E, Álvarez R M S, Structural modifications induced by an in vitro maturation process in zona pellucida glycoproteins of bovine oocytes. A Raman microspectroscopy análisis, *RSC Adv*, 6(2016)83429–83437.
34. Berton A, Godeau G, Emonard H, Baba K, Bellon P, Hornebeck W, Bellon G, Analysis of the ex vivo specificity of human gelatinases A and B towards skin collagen and elastic fibers by computerized morphometry, *Matrix Biol*, 19(2000)139–148.
35. Vogel B, Siebert H, Hofmann U, Frantz S, Determination of collagen content within picrosirius red stained paraffin-embedded tissue sections using fluorescence microscopy, Methods X, 2(2015)124–134.
36. Dayan D, Hiss Y, Hirshberg A, Bubis J J, Wolman M, Are the polarization colors of Picrosirius red-stained collagen determined only by the diameter of the fibers?, *Histochemistry*, 93(1989)27–29.
37. Montes G S, Junqueira L C U, The use of the Picrosirus-polarization method for the study of the biopathology of collagen, *Mem Inst Oswaldo Cruz*, 86(1991)1–11.
38. Sexton O J, Veith G M, Phillips D M, Ultrastructure of the eggshell of two species of anoline lizards, *J Exp Zool*, 207(1979)227–236.
39. Chang Y, Chen P Y, Hierarchical structure and mechanical properties of snake (Naja atra) and turtle (Ocadia sinensis) eggshells, *Acta Biomater*, 31(2016)33–49.
40. Kodali V K, Gannon S A, Paramasivam S, Raje S, Polenova T, Thorpe C, A novel disulfide-rich protein motif from avian eggshell membranes, *PloS One*, 6(2011)1–11.
41. Revell C K, Jensen O E, Shearer T, Lu Y, Holmes D F, Kadler K E, Collagen fibril assembly: New approaches to unanswered questions, Matrix Biol Plus, 12(2021)100079; doi.org/10.1016/j.mbplus.2021.100079.
42. Al Makhzoomi A K, Kirk T B, Dye D E, Allison G T, Contribution of glycosaminoglycans to the structural and mechanical properties of tendons - A multiscale study, *J Biomech*, 128(2021)110796; doi.org/10.1016/j.jbiomech.2021.110796.
43. Jimenez L E, Roldán-Olarte M, Álvarez R M S, Raman Microscopy Analysis of the Biochemical Changes in the Cytoplasm of Bovine Oocytes Induced by an *In Vitro* Maturation Process: Interference of the Zona Pellucida, ChemistrySelect, 4(2019)3706 –3716.
44. Kuzuhara A, Fujiwara N, Hori T, Analysis of internal structure changes in black human hair keratin fibers with aging using Raman spectroscopy, *Biopolymers*, 87(2007)134–140.
45. Essendoubi M, Meunier M, Scandolera A, Gobinet C, Manfait M, Lambert C, Auriol D, Reynaud R, Piot O, Conformation changes in human hair keratin observed using confocal Raman spectroscopy after active ingredient application, *Int J Cosmet Sci*, 41(2019)203–212.
46. Garcia Martinez M, Bullock A J, MacNeil S, Rehman I U, Characterisation of structural changes in collagen with Raman spectroscopy, *Appl Spectrosc Rev*, 54(2019)509–542.
47. Bonifacio A, Beleites C, Vittur F, Marsich E, Semeraro S, Paoletti S, Sergo V, Chemical imaging of articular cartilage sections with Raman mapping, employing uni- and multi-variate methods for data analysis, *Analyst*, 135(2010)3193–3204.
48. Feng X, Fox M C, Reichenberg J S, Lopes F C P S, Sebastian K R, Markey M K, Tunnell J W, Biophysical basis of skin cancer margin assessment using Raman spectroscopy, *Biomed Opt Express*, 10(2019)104; doi.org/10.1364/boe.10.000104.
49. Nguyen T T, Gobinet C, Feru J, Brassart-Pasco S, Manfait M, Piot O, Characterization of type I and IV collagens by Raman microspectroscopy: Identification of spectral markers of the dermo-epidermal junction, *Spectrosc Int J*, 27(2012)421–427.
50. Cárcamo J J, Aliaga A E, Clavijo R E, Brañes M R, Campos-Vallette M M, Raman study of the shockwave effect on collagens, *Spectrochim Acta*, 86A(2012)360–365.
51. Rintoul L, Carter E A, Stewart S D, Fredericks P M, Keratin orientation in wool and feathers by polarized Raman spectroscopy, *Biopolymers*, 57(2000)19–28.

52. Bazylewski P, Divigalpitiya R, Fanchini G, *In situ* Raman spectroscopy distinguishes between reversible and irreversible thiol modifications in l-cysteine, *RSC Advances*, 7(2017)2964–2970.
53. Alimova A, Chakraverty R, Muthukattil R, Elder S, Katz A, Sriramoju V, Lipper S, Alfano R R, (2009). In vivo molecular evaluation of guinea pig skin incisions healing after surgical suture and laser tissue welding using Raman spectroscopy, *J Photochem Photobiol B Biol*, 96(2009)178–183.
54. Kim J, Feng J, Jones C A R, Mao X, Sander L M, Levine H, Sun B, Stress-induced plasticity of dynamic collagen networks, *Nat Commun*, 8(2017)842; doi.org/10.1038/s41467-017-01011-7.
55. Trauth S E, Fagerberg W R, Ultrastructure and stereology of the eggshell in Cnemidophorus sexlineatus (Lacertilia: Teiidae), *Copeia*, (1984)826–832; doi.org/10.2307/1445324.
56. Trauth S E, McAllister C T, Chen W, Microscopic eggshell characteristics in the Collared Lizard, Crotaphytus collaris (Sauria: Crotaphytidae), *Southwest Nat*, 39(1994)45–52.
57. Grolik M, Szczubialka K, Wowra B, Dobrowolski D, Orzechowska-Wylegala B, Wylegala E, Nowakowska M, Corneal epithelial scaffolds based on chitosan membranes containing collagen and keratin, *Int J Polym Mater*, 64(2014)140–148.

[*Received*: 03.12.2021; *revised recd*: 01.01.2022; *accepted*: 12.01.2022]

Rosa María Susana Álvarez (e-mail: maria.alvarez@fbqf.unt.edu.ar)

María Álvarez is a Professor at the Faculty of Biochemistry, Chemistry and Pharmacy of the National University of Tucumán, Argentina and a Researcher at the National Council for Scientific and Technical Research (CONICET). She received her PhD degree in Chemistry from the National University of Tucumán in 1997. Since then her interest has focused on the study of different types of chemical and biological systems using Raman spectroscopy. She did postdoctoral stays with DAAD fellowships at the University of Bremen to synthesize and vibrationally study fluorinated compounds and at the Max Planck Institute for Chemical Energy Conversion in Mülheim an der Ruhr where she studied the effect of thyroid hormones in lipid membranes. She made other stays at the University of Tübingen (2000), University of Málaga (2005); University of Pittsburgh (2008), and University of San Diego (2012), where she perfected herself in the application of UV-Raman spectroscopy and Raman microscopy. She has published several articles in specialized vibrational spectroscopy journals. Currently her interest is focused on the characterization of the biochemical components of complex biological systems.

Alfredo Nicolás Dominguez (e-mail: nicolas9414@gmail.com)

Nicolás Dominguez is a PhD student at the Institute of Chemistry of Northwest Argentina. His thesis work is about the detection of pesticides in lemon using surface enhanced Raman spectroscopy (SERS) as ultrasensible method. He received his degree in biotechnology from National University of Tucumán, Tucumán, Argentina, in 2017. He is also currently an Instructor of Organic Chemistry at the National University of Tucuman.

Francisco Alejandro Cortez (e-mail: franchocortez@gmail.com)

Francisco Cortez is a Zootechnics Engineer and is currently a Professor at at the Faculty of Agronomy and Zootechnics, National University of Tucumán, Argentina. He has experience in breeding and management of tegu lizards in captivity. Currently, his work is focused on eggshell biomaterials from the eggshell of the Salvator merianae.

Oscar Augusto Carlino-Aráoz (e-mail: osau88@gmail.com)

Augusto Carlino-Aráoz is an advanced student of Veterinary Medicine and a research fellow of the National Council of Universities (CIN) of Argentina. He is also currently an Assistant of Veterinary Histology at the Faculty of Agronomy and Zootechnics, National University of Tucumán, Argentina.

Fernando Campos-Casal (e-mail: fhccasal@gmail.com)

Fernando Campos-Casal is a Professor of Developmental Biology at the Faculty of Agronomy and Zootechnics, National University of Tucumán, Argentina. He completed his undergraduate course in Biological Sciences and received a Ph D degree in Biological Sciences (Zoology) in 1999, both from the Natural Sciences Faculty of the Universidad Nacional de Tucumán. Initially his research was focused on the study of cytoplasmic determinants and cellular interactions involved in mesodermal layer regionalization. He is currently a representative before the National Biotherium System of the Salvator Lizard Hatchery of the Faculty of Agronomy and Zootechnics and his studies include the study of eggshell biomaterials in reptile species.